

The Analysis of Numerical Simulation Method for Convection Heat Transfer of Water under Complex and Supercritical Conditions

Jun Li, Xusheng Zhai, Gang Li and Ping Xie

Air Force Engineering University Aviation Maintenance NCO Academy, Xinyang, Henan, 46400, China.

Email: hitlijun1989@163.com

Keywords: Supercritical; Convective heat transfer; Numerical Simulation; Turbulence model

Abstract: Taking the convective heat transfer process of supercritical water in vertical tubes as the research object, the effects of different turbulence models on numerical simulation, the reliability of calculation results, the accuracy of numerical simulation under complex conditions, and the characteristics of heat transfer in tubes were studied. In this paper, a turbulence model with high calculation accuracy is selected to numerically simulate the flow and heat transfer of water in a vertical pipe under complicated working conditions. The calculation results are compared with the existing experimental data, and the calculation results of the turbulence model under complicated conditions are analyzed. Extract the axial and radial physical properties parameters, and study its influence on heat transfer by analyzing its variation law, compared with the research of heat transfer characteristics in the tube; there will be obvious temperature gradients in the tube heat transfer, so the axial and vertical temperature are extracted. The cloud map analyzes the change law of the temperature field and finds its effect on the flow and heat transfer in the tube.

The drastic changes in physical properties with pressure and temperature are the main characteristics of fluid flow and heat transfer in the tube under supercritical pressure. Especially near the quasi-critical point, the physical properties change extremely drastically. This drastic change in physical properties under supercritical pressure will inevitably have a great effect on the convective heat transfer of the fluid in the tube. Due to this change, under different circumstances, the heat transfer of supercritical water in the tube will be more complicated, and heat transfer enhancement and deterioration may occur. However, due to the limitation of experimental conditions, the test data can only obtain the temperature at the wall surface. Then the heat transfer coefficient is deduced. These parameters are not enough to help us fully understand the flow and heat transfer in the tube. Therefore, we need to find a method that can explore the heat transfer characteristics in the tube. Heat provides convenience.

1. The Choice of Turbulence Calculation Model

In order to select a suitable turbulence calculation model, three turbulence models were first used to simulate the convective heat transfer in a supercritical water vertical tube under the working condition 1. See Table 1 for the working conditions.

Table 1 Calculation conditions

No	Pipe diameter /mm	Inlet temperature /°C	pressure /MPa	Mass Flow /kg/m ² s	Heat flux /W/m ²
Case1	10	300.5	25	597.81	573222
Case2	10	294.1	25	1189.15	1160175

Comparing the calculation results with the experimental results, it is found that when the SSTk-w turbulence calculation equation is used for three-dimensional numerical calculation, the heat transfer deterioration region in the tube, that is, the abrupt region of the wall temperature, can be predicted, but the predicted value is wrong than the experimental data. Large, more than 30%,

can be used for qualitative analysis; while the calculation results of the $k-\varepsilon$ and RNG $k-\varepsilon$ turbulence calculation equations in the heat transfer deterioration region are poor, the overall prediction accuracy is better than SST $k-\omega$ turbulence. The model is high and the error range is within 30%. As a whole, the 3D numerical simulation results are more accurate than the 2D simulation results. The error range for 2D calculations exceeds 50%. Therefore, it is necessary to consider whether the dimensions of the model can meet the calculation requirements when performing numerical calculations.

This paper chooses to use $k-\varepsilon$ and RNG $k-\varepsilon$ turbulence models to simulate the flow and heat transfer under complex conditions. On the one hand, it further analyzes the differences in numerical simulation of $k-\varepsilon$ and RNG $k-\varepsilon$ turbulence models to understand the results of their numerical simulation Applicability; on the other hand, through numerical simulation, the mechanism and characteristics of supercritical water flow and heat transfer in vertical tubes under complex working conditions are investigated. This paper uses two turbulence models to calculate the results under the conditions of variable mass flow and heat flux density for simulation analysis.

In this calculation, FLUENT software was used to add the boundary layer to encrypt the mesh at the liquid-solid coupling. The coupling relationship between processing speed and pressure uses the SIMPLE algorithm; the governing equations include continuity equations, momentum equations, and energy equations; the inlet is set as the mass flow inlet, the outlet is the pressure outlet, and the wall is set as the heat flow wall surface with constant heat flow density.

2. With High Quality Flow and Thermal Density, $k-\varepsilon$ Simulation Analysis of Turbulence Model

2.1. Wall surface temperature analysis

The selected high-quality flow calculation conditions are shown in Table 1 and Condition 2.

Table 1 Comparison of calculation conditions

No	Pipe diameter /mm	Inlet temperature /°C	Pressure /MPa	Mass Flow /kg/m ² s	Heat flux /W/m ²
Case1	10	300.5	25	597.81	573222
Case2	10	294.1	25	1189.15	1160175

It can be seen from the table that the mass flow rate and heat flux density have changed in comparison with working conditions 1 and 2, and the inlet temperature has also changed to some extent, but the difference is not large. Analyze the calculation results, extract the wall surface temperature of the pipeline as shown in Table 2, and make the wall surface temperature curve as shown in Figure 1.

Table 2 Wall temperature of the pipeline

Pipe location /m	$RNGk - \varepsilon$ Turbulence model wall temperature /K
0	567.1
0.12	567.1
0.24	567.1
0.36	567.1
0.48	567.1
0.6	630.704
0.72	642.018
0.84	652.881
0.96	661.421
1.08	670.804
1.2	678.042
1.32	681.941
1.44	681.643
1.56	680.212
1.68	682.961
1.8	689.202
1.92	714.406
2.04	752.383
2.16	791.907
2.28	830.845
2.4	894.757
2.52	923.677
2.64	924.498
2.76	895.257
2.88	878.157
3	778.439

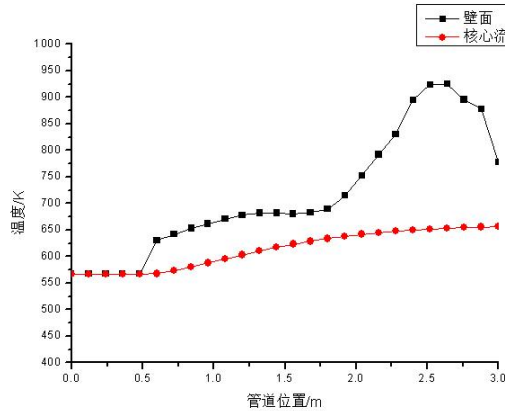


Figure 1 Wall temperature

From the wall temperature curve, it can be seen that for the effect of the wall entrance section, the first 0.5 meters is an adiabatic section and enters the heating section from 0.5 meters. With the flow of water in the pipe, the wall temperature rises rapidly to 650K at 0.6 meters. The wall temperature gradually increased. When the pipe reached 1.2 meters, the temperature inside the pipe reached about 680K. At this time, the rising temperature of the pipe wall had weakened to a certain extent, reaching 690K at 1.8 meters, and then the rising trend accelerated, rising at 2.5 meters. At about 950K, the wall temperature was basically the maximum at this time, and then the wall temperature began to drop at 2.6 meters. Near the exit, the wall temperature of the pipe accelerated to fall back to about 778K.

The temperature change trend at the core flow can be seen that after the water enters the heating section, the temperature gradually rises. After the water in the tube reaches 2 meters, the temperature rises to 640K. After that, the wall temperature rise tends to stabilize, and the core flow temperature at the outlet. Only rose to about 650K.

Comparing the calculation results of the numerical simulation with the experimental data of Wang Lei and others, it can be seen that the overall wall temperature change trend is basically the same. The specific analysis shows that the wall temperature at the middle and early stages of entering the heating section basically accorded with the experimental data, and a difference

appeared after entering 1 meter. The wall temperature calculated by numerical simulation is lower than the experimental data, at 1.8 meters. The difference is close to 50K. After that, the wall temperature calculated by numerical simulation increased rapidly, and the upward trend was faster than the experimental data. At 2.5 meters, the calculated value exceeded the experimental data by 70K, and then the difference between the two gradually decreased. At the exit, the numerical calculation The wall temperature value dropped to 800K. At this time, the error with the experimental data reached 70K, and the error range was more than 5% and not more than 10%.

By comparing the calculation results of the numerical simulation with the experimental data, it can be found that the results of the numerical simulation and the data fit well in the front end, the error in the second half is large, and the prediction of the wall temperature rising stage is not accurate. The predicted wall temperature rise time is later than the experimental data, the rising speed is faster than the experimental data, and the maximum wall temperature is also 8% higher than the experimental data. , But not more than 10%.

2.2. Analysis of axial parameters

In order to analyze the cause of the wall temperature change, the physical property parameters of the fluid at the wall surface in the axial direction are extracted and analyzed.

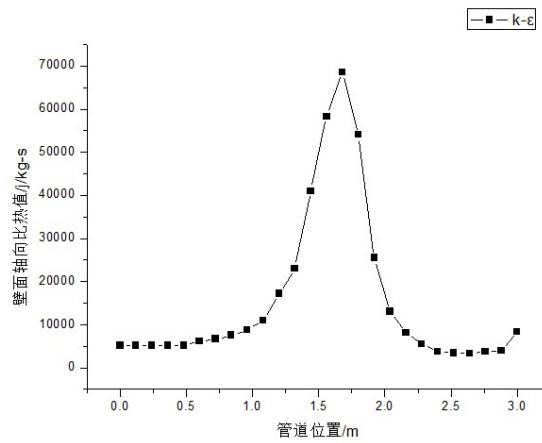


Figure 2 Axial specific heat value distribution

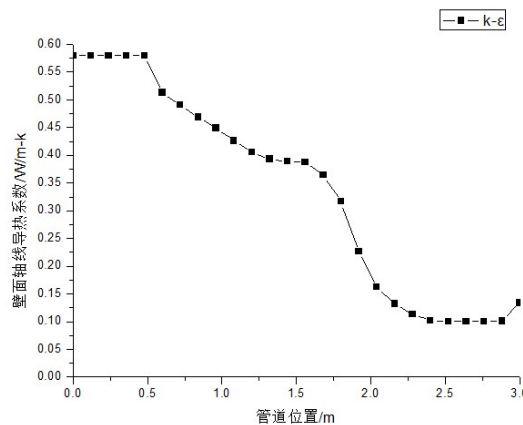


Figure 3 Axial thermal conductivity distribution

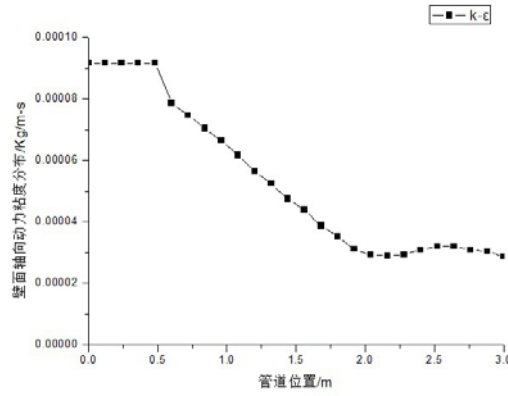


Figure 4 Axial dynamic viscosity distribution

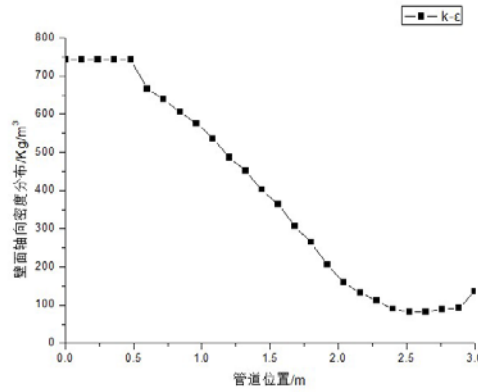


Figure 5 Axial density distribution

From the diagrams in the four figures above, it can be seen that in the adiabatic section, the axial parameters of the fluid at the wall surface have not changed. At this stage, the influence of the inlet section is weakened when water flows in the tube. After entering the heating section, the physical parameters follow the tube. The rise in fluid temperature changes.

Figure 2 shows the distribution of the axial specific heat value of the fluid at the wall surface. It can be seen from the figure that when the water enters the heating section in the pipe, the specific heat value gradually increases as the wall temperature gradually rises, and the heat absorption capacity of the water increases. When the water reaches 1.2 meters in the pipe, the specific heat value at the wall of the pipe starts to rise sharply. It can be known from the physical property curve that the temperature of the water here is close to the critical temperature, and the specific heat value changes dramatically, ranging from 1.2 meters to 1.6 meters. The specific heat value increased from 10000j / kg-s to 70,000j / kg-s. The specific heat value showed a geometric exponential increase at this stage. The sharp rise in specific heat value caused the heat absorbed by the water from the wall surface to increase. As the wall temperature rises further, the specific heat value exhibits a geometric exponential decrease after entering the supercritical region, and decreases to 5000 j / kg-s at 2.2 meters. After that, the specific heat value changes little and tends to stabilize. There was a certain increase in specific heat value at 2.9 meters.

The distribution of the thermal conductivity of the fluid at the wall in Figure 3 shows that after entering the heating section, the thermal conductivity drops abruptly from 0.5 to 0.6 meters as the wall temperature rises, from 0.57 W / mK to 0.51 W / mK, after which the declining trend slows down, the thermal conductivity gradually decreases to 0.375W / mK at 1.5 meters, and the thermal conductivity decreases rapidly after 1.5 meters, and the thermal conductivity decreases from 0.375 W / mK to 1.5 meters to 2.1 meters 0.15 W / mK, after which the thermal conductivity tends to be stable, dropping to 0.10 W / mK at 2.9 meters, and there is a certain increase in value at the exit.

It can be seen in the dynamic viscosity distribution chart in FIG. 4 that after entering the heating section, the dynamic viscosity changes linearly with the increase of wall temperature, from 9.1E-05kg / ms at 0.5 meters to 2 meters 3E-05kg / ms, and then there is a weak upper body at 0.5

meters, and the dynamic viscosity at the exit is $3\text{E-}05\text{kg / ms}$. The distribution of the axial density of the fluid at the wall in Figure 5 and the distribution trend of the dynamic viscosity are basically the same. The density value ranges from 750kg / m^3 when it first enters the heating section to about 100 kg / m^3 at 2.5 meters, and then there is a certain The rise at the exit is about 150 kg / m^3 . The rise in density also reflects the decrease in wall temperature here.

Combining the wall temperature curve, it can be seen that as the heat absorbed by the water in the pipe increases, the temperature of the fluid at the wall rises. As the temperature rises, the physical properties of the fluid also change. When the fluid temperature reaches a critical temperature, the physical properties enter a region of drastic change. . Dramatic changes in physical properties will also affect the heat transfer of water in the tube. The increase in the specific heat value of water will cause the heat absorbed by the water to increase rapidly from the wall temperature curve. It can be seen from the wall temperature curve that the wall temperature value is 1.5 meters at the stage of the pipeline. Basically kept constant, the upward trend is very small, but the corresponding increase in the heat absorption causes the water temperature to rise rapidly. Due to the decrease in the thermal conductivity, the heat absorbed by the fluid at the wall surface cannot be transferred to the fluid at the core in time. It means that the heat of the fluid at the wall surface cannot be taken away in time. During the forward flow of the fluid at the wall surface, due to the temperature rising to a certain degree, the heat absorbed from the wall surface will decrease sharply. Take away the absorbed heat in time. As a result, the temperature of the viscous bottom layer of the wall surface will rise sharply in the second half, and the wall surface will become hot. The decrease in the wall temperature at the outlet may be due to the decrease in viscosity and density, which increases the speed of the fluid at the core. At this time, the specific heat of water has decreased, and the ability to absorb heat from the wall surface has stabilized, and the fluid at the wall surface will not collect a large amount of fluid. The amount of heat that cannot be taken away, and the specific heat value and thermal conductivity have risen here. The ability of the core fluid to take away heat from the fluid at the wall surface has increased, so the wall temperature at the outlet has decreased.

2.3. Radial parameter analysis

In order to visually analyze the heat transfer in the tube, the radial parameters at $L = 1.1$ meters and $L = 2.5$ meters are extracted for analysis, as shown in Figures 6 to 11.

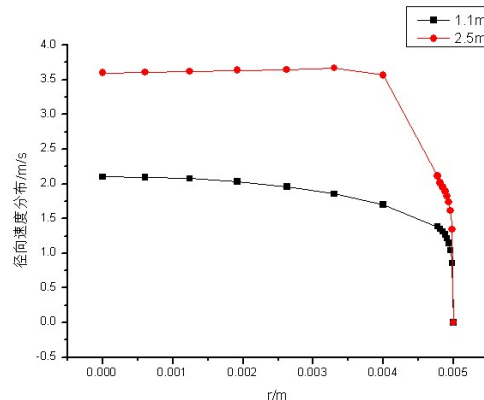


Figure 6 Radial velocity distribution

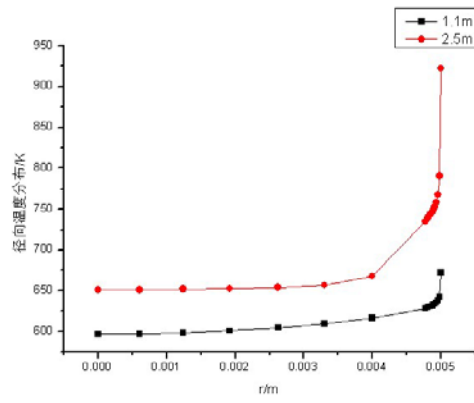


Figure 7 Radial temperature distribution

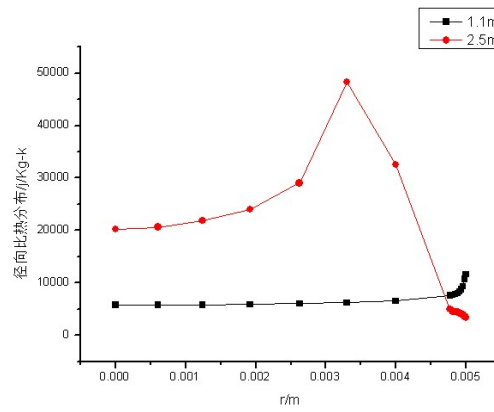


Figure 8 Radial specific heat distribution

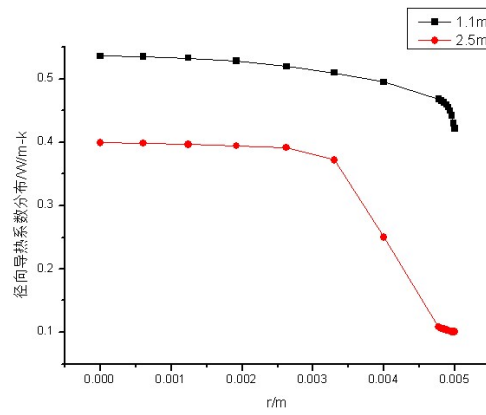


Figure 9 Radial thermal conductivity distribution

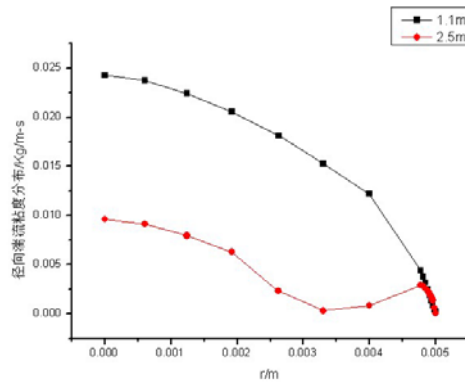


Figure 10 Radial turbulent viscosity distribution

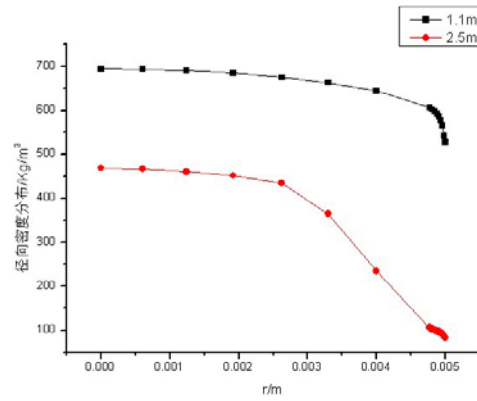


Figure 11 Radial density distribution

It can be seen from the radial velocity distribution diagram in FIG. 6 that in the axial direction, as the fluid continues to flow, the fluid velocity in the tube gradually rises. In the radial direction, the fluid velocity at the core is the highest, and the velocity gradually decreases in the radial direction. When the velocity is 1mm away from the wall surface, the velocity decreases sharply until the wall surface reaches zero. At $L = 1.1$ meters, the temperature of water decreases sharply only 0.2mm near the wall surface. It can be seen that when the wall temperature rises sharply and the heat transfer in the tube deteriorates, the boundary layer at the wall surface has thickened and the wall surface Thickening of the layer will reduce the heat transfer effect.

Observing the radial temperature distribution of the fluid in Figure 7, it can be seen that the thermal temperature difference in the radial direction is mainly concentrated on the viscous bottom layer. At $L = 2.5$ meters, the radial temperature also rises sharply at 1mm from the wall surface, and the temperature reaches the highest at the wall surface. The radial temperature trend at $L = 1.1$ meters is basically the same as that at $L = 2.5$ meters. The area where the temperature changes at $L = 1.1$ meters is about 0.2mm near the wall surface. This change is consistent with the point where the radial velocity changes.

It can be seen that the specific heat value distribution in the radial direction in FIG. 8 shows that the specific heat value at 2.5 meters in the core flow region is significantly higher than the specific heat value at 1.1 meters. This is also because the temperature of the mainstream of the fluid rises and enters the critical region. The distribution curve of the radial specific heat value at $L = 2.5$ meters shows an M-type. When the viscous bottom layer near the wall surface reaches the maximum value, the specific heat value decreases sharply after that, mainly due to the existence of a large internal viscous bottom layer. The temperature gradient makes the physical properties change drastically. The radial specific heat at $L = 1.1$ meters only shows a large change gradient when it is about 0.2mm away from the wall surface, which is also because the adhesive bottom layer is thinner here.

It can also be seen from Figure 9 that in the radial direction, the thermal conductivity gradually decreases and reaches the lowest value at the wall surface. The difference in radial thermal conductivity is also mainly concentrated in the fluid at the wall surface, which is mainly due to the radial temperature of the fluid Caused by the radial distribution law. The existence of a viscous bottom layer near the wall surface area causes a sharp rise in temperature, the existence of a temperature gradient causes a large gradient of thermal conductivity, and a decrease in thermal conductivity makes the heat transfer capacity between the fluids in the tube weaken.

The radial distribution of turbulent viscosity in Fig. 10 shows that the axial turbulent viscosity gradually decreases, while in the radial direction, it gradually decreases from the center to the radial direction, the wall surface reaches the minimum value, the turbulent viscosity decreases, and the radial turbulent flow energy Will reduce, so that the radial mixing heat transfer capacity is reduced. It can be seen from the radial distribution of density in Figure 11 that the density at $L = 2.5$ m is significantly smaller than the fluid density at $L = 1.1$ m. The distribution pattern of radial density is still parabolic, and the high temperature at the wall makes the density relatively Smaller.

3. Under the Condition of High Quality Flow and Heat Flux Density, $RNGk - \varepsilon$ Simulation Analysis of Turbulence Model

3.1. Wall surface temperature analysis

Use this model to carry out numerical simulation of Case2, analyze the calculation results, extract the wall temperature of the pipeline as shown in Table 3 below, and make the wall temperature curve as shown in Figure 12.

Table 3 Pipe wall temperature

Pipe location /m	$RNGk - \varepsilon$ Wall temperature of turbulence model/K
0	567.1
0.12	567.1
0.24	567.1
0.36	567.1
0.48	567.1
0.6	628.533
0.72	647.474

Table 3 (continued)

Pipe location /m	$RNGk - \varepsilon$ Wall temperature of turbulence model/K
0.84	681.014
0.96	677.046
1.08	669.772
1.2	676.532
1.32	680.874
1.44	682.571
1.56	681.249
1.68	680.86
1.8	684.224
1.92	696.486
2.04	746.005
2.16	845.267
2.28	932.938
2.4	934.873
2.52	927.259
2.64	941.215
2.76	948.129
2.88	942.98
3	924.076

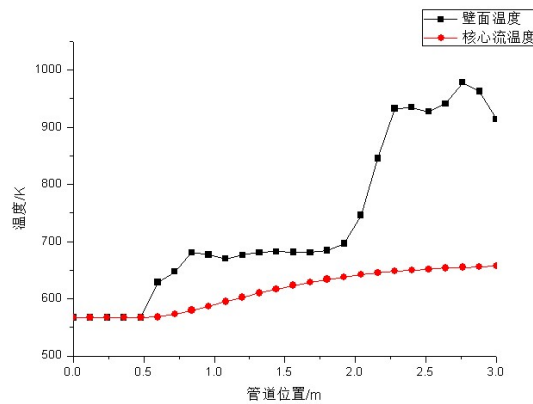


Figure 12 $RNGk - \varepsilon$ Wall temperature of the model

From the wall temperature curve, it can be seen that for the effect of the wall inlet section, the first 0.5 meters is an adiabatic section and enters the heating section from 0.5 meters. With the flow of water in the pipe, the wall temperature is rising rapidly, rising to 0.8 meters at Nearly 680K, the temperature of the wall dropped again, then dropped to 650 at 1 meter, then the temperature of the

wall rose slowly, reaching 690K at 1.8 meters, and then the upward trend accelerated, rising to about 930K at 2.5 meters, at 2.8 meters It rises to about 940K, which is basically the maximum value of the wall temperature, and then the wall temperature starts to drop at 2.8 meters. Near the exit, the wall temperature of the pipe accelerates to fall back to about 920K.

The temperature change trend at the core flow can be seen that after the water enters the heating section, the temperature gradually rises. After the water in the tube reaches 2 meters, the temperature rises to 640K. After that, the temperature rise of the wall surface stabilizes. Only rose to about 655K.

Comparing the calculation results of the numerical simulation with the experimental data of Wang Lei and others, it can be seen that the overall wall temperature change trend is basically the same. The specific analysis shows that the wall temperature at the initial stage of entering the heating section basically accords with the experimental data, and a difference occurs after entering 1 meter. The wall temperature calculated by numerical simulation is lower than the experimental data, and the difference is 1.8 meters The value is close to 50K. Later, the wall temperature calculated by numerical simulation increased sharply, and the experimental data showed a clear upward trend after 2 meters, and the upward trend was slow. When the result of numerical simulation calculation was 2.5 meters, it exceeded the experimental data by 70K. The difference between them gradually decreased. At the exit, the numerically calculated wall temperature value dropped to 930K. At this time, the error with the experimental data reached 60K, and the error range exceeded 5%, and did not exceed 10%.

By comparing the calculation results of the numerical simulation with the experimental data, it can be found that the results of the numerical simulation and the data fit well in the front end, the error in the second half is large, and the prediction of the wall temperature rising stage is not accurate. The predicted wall temperature rise time is later than the experimental data, the rising speed is faster than the experimental data, and the maximum wall temperature is also 8% higher than the experimental data. , But not more than 10%.

3.2. Analysis of axial parameters

The axial physical properties of the fluid at the wall are extracted and plotted as shown in Figures 13 to 16.

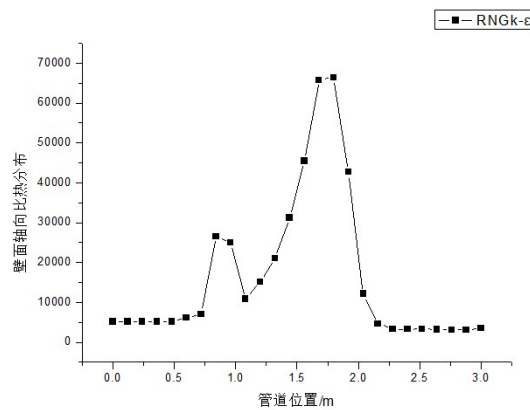


Figure 13 Axial specific heat distribution

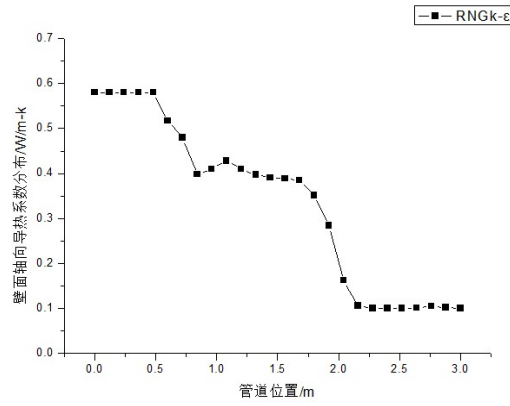


Figure 14 Axial thermal conductivity distribution

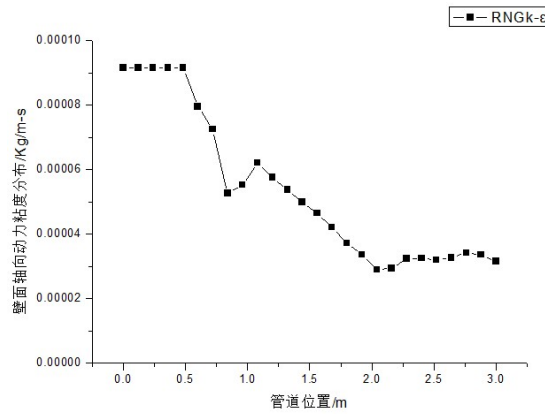


Figure 15 Axial dynamic viscosity distribution

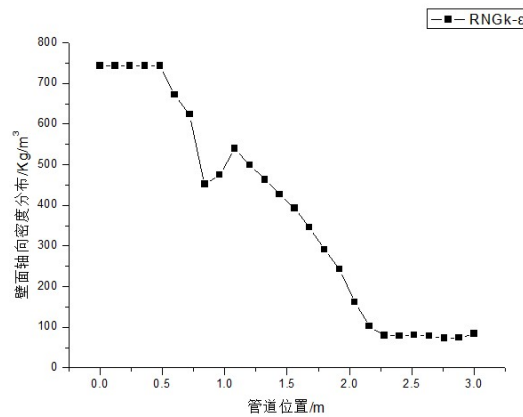


Figure 16 Axial density distribution

It can be seen from the above four figures that the overall change trend of physical property parameters is similar to the change law of fluid axial physical property parameters at the wall surface calculated by the k-ε turbulence model.

Figure 13 shows the axial specific heat value distribution of the fluid at the wall surface. It can be seen from the figure that when the water enters the heating section in the pipe, the specific heat value gradually increases with the gradual rise of the wall temperature, and the heat absorption capacity of the water increases at this time. When the water reaches 0.8 meters inside the pipe, there is a sudden change in the specific heat value, which rises to 30000j / kg·s, and then drops to 12000j / kg·s, after which the specific heat value rises again, and rises to 70,000j / kg at 1.8 meters. -s, the specific heat value exhibits a geometric exponential growth at this stage. The sharp rise of the specific heat value causes the heat absorbed by the water from the wall surface to increase. After that, as the wall temperature further increases, the specific heat value enters the supercritical zone.

The value showed a geometric exponential decline, which decreased to 5000 J / kg-s at 2.2 meters, and then the specific heat value changed little and tended to be stable.

The distribution of fluid thermal conductivity at the wall surface in Figure 14 shows that after entering the heating section, the thermal conductivity drops abruptly from 0.5 to 0.8 meters as the wall temperature rises, from 0.57 W / mK to 0.38 W / mK, rises to 0.45 W / mK at 1.1 meters, and then decreases gradually, the thermal conductivity gradually decreases to 0.4 W / mK at 1.5 meters, and the thermal conductivity decreases after 1.5 meters to 1.5 meters to 2.1 The thermal conductivity at meters decreased from 0.4 W / mK to 0.1 W / mK, after which the thermal conductivity became stable.

It can be seen from the dynamic viscosity distribution chart in Fig. 15 that the distribution law is basically similar to the distribution law of thermal conductivity. After entering the heating section, as the wall temperature rises, the dynamic viscosity decreases sharply, from 9.1E-05kg / ms at 0.5 meters It reached 5E-05kg / ms at 0.8 meters, then rose to 6.3 E-05kg / ms at 1.1 meters, and then the downward trend was linear. At 2 meters, the dynamic viscosity decreased to 3E-05kg / ms. In the distance from 2 meters to the exit, the dynamic viscosity varies from 3E-05kg / m-s to 4E-05kg / m-s, and the exit is 3.2E-05kg / m-s.

The distribution value of the axial density of the fluid at the wall surface in Figure 16 and the distribution trend of the dynamic viscosity are basically the same. The density value decreased from 750kg / m³ immediately after entering the heating section to about 450kg / m³ at 0.8 meters. Ascent, it rises to about 560 kg / m³ at 1.1 meters. From 1.1 meters to 2.1 meters, the downward trend of the density value is basically linear, at 2.1 meters to 100 kg / m³. The density value was basically stable after that.

From the overall analysis of the axial parameter curve, it can be seen that there is an abnormal change in physical properties at a distance of 0.8 meters from the inlet. This is mainly because the temperature at the wall is close to the critical temperature, and a small temperature fluctuation will accompany the severe physical properties Changes, so there will be sharp fluctuations in physical properties.

Combining the wall temperature curve, it can be seen that as the heat absorbed by the water in the pipe increases, the temperature of the fluid at the wall rises. As the temperature rises, the physical properties of the fluid also change. When the fluid temperature reaches a critical temperature, the physical properties enter a region of drastic change. . Dramatic changes in physical properties will also affect the heat transfer of water in the tube. The increase of the specific heat value of water will increase the heat transfer coefficient of water, and the heat absorbed from the wall surface will increase rapidly. Therefore, the wall temperature curve remains basically constant at 1.5 meters of the pipeline, and the upward trend is small. However, with the increase in heat absorption, the water temperature rises rapidly. When the temperature exceeds the critical region and enters the supercritical range, the physical property changes tend to stabilize. At this time, the decrease in specific heat value causes the heat transfer coefficient to decrease, and the thermal conductivity coefficient to decrease. It is also that the heat of the fluid accumulated on the wall cannot be transferred to the fluid in the core in a timely manner, which means that the heat of the fluid on the wall cannot be taken away in time, and the heat absorbed by the wall will decrease sharply, which results in the second half of the pipeline The temperature of the viscous bottom layer on the wall will rise sharply, the heat transfer effect will be weakened, and the wall temperature will become high.

3.3. Radial parameter analysis

The existence of radial parameters can more clearly recognize the heat transfer situation in the tube and the change of physical properties. Therefore, the radial parameters at $L = 1.1$ m and $L = 2.5$ m in the tube were extracted for analysis. The parameter distribution rules are shown in Figures 17 to 22.

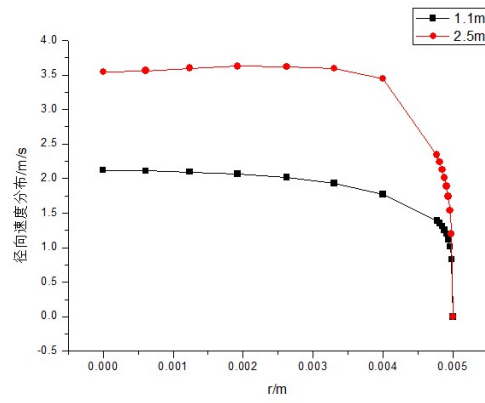


Figure 17 Radial velocity distribution

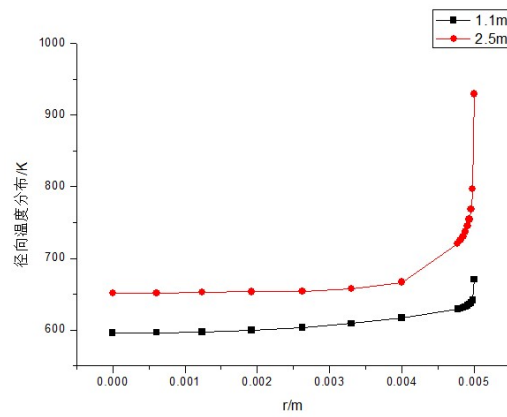


Figure 18 Radial temperature distribution

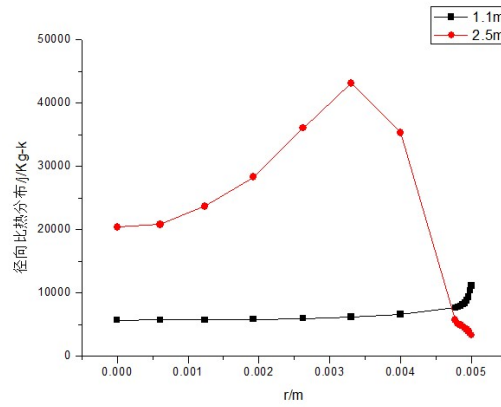


Figure 19 Radial specific heat distribution

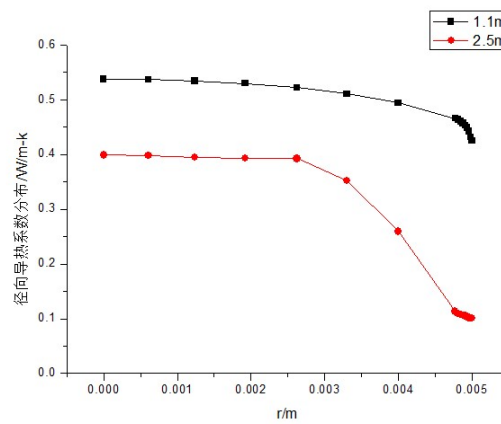


Figure 20 Radial thermal conductivity distribution

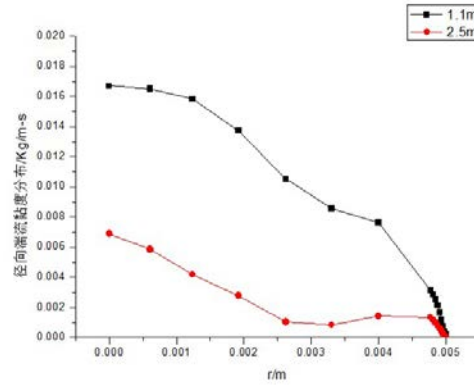


Figure 21 Viscosity distribution of radial turbulence

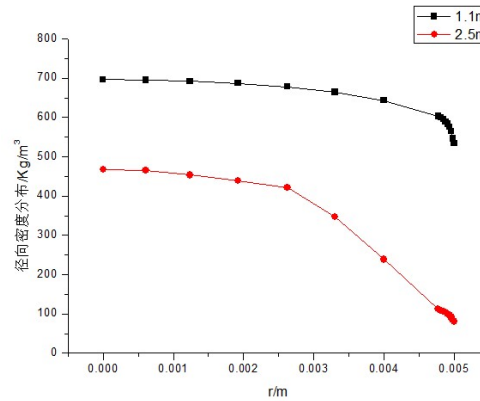


Figure 22 Radial density distribution

From the distribution of radial velocity in Fig. 17, it can be seen that along the axial direction, as the fluid in the pipe flows, the fluid velocity gradually increases. In the radial direction, the water temperature decreases sharply at $L = 2.5$ m and $r = 4$ mm. Until the velocity drops to zero at the wall. At $L = 1.1$ meters, the temperature of water drops sharply at $r = 4.8$ mm. It can be seen that when the wall temperature rises sharply and the heat transfer in the tube deteriorates, the boundary layer at the wall has thickened and the wall surface Thickening of the layer will reduce the heat transfer effect.

Observing the radial temperature distribution of the fluid in Figure 18, it can be seen that the thermal temperature difference in the radial direction is mainly concentrated on the viscous bottom layer. At $L = 2.5$ meters, the radial temperature also rises sharply at $r = 4$ mm, and the temperature reaches the highest at the wall surface. The radial temperature change trend at $L = 1.1$ meters is basically the same as that at $L = 2.5$ meters. The difference is L The area where the temperature changes at 1.1 meters is about $r = 4.8$ mm. This change is consistent with the point where the radial velocity changes.

It can be seen that the specific heat value distribution in the radial direction in FIG. 19 shows that the specific heat value at 2.5 meters in the core flow region is significantly higher than the specific heat value at 1.1 meters. This is also because the temperature of the fluid main stream rises. When the distribution curve of the radial specific heat value at $L = 2.5$ m is at $r = 3.5$ mm, the specific heat value appears at the maximum value, and then the specific heat value decreases sharply, mainly due to the large temperature gradient inside the viscous bottom layer and the wall surface. The fluid at the site enters the supercritical region, and the specific heat value decreases sharply. The radial specific heat at $L = 1.1$ meters only shows a large change gradient when it is about 0.2 mm away from the wall surface. The change here is similar to the radial velocity and temperature change.

It can also be seen from FIG. 20 that along the axial direction, as the fluid flows, the thermal conductivity gradually decreases. In the radial direction, there is a difference in the radial distribution of thermal conductivity between $L = 1.1$ m and $L = 2.5$ m. The radial difference at 2.5 meters is significantly higher than the value at 1.1 meters. The difference in radial heat conduction

is also mainly on the wall the interior of the fluid is mainly caused by the existence of a large temperature gradient in the radial direction. The existence of a viscous bottom layer near the wall surface area causes a sharp rise in temperature, the existence of a temperature gradient causes a large change gradient in thermal conductivity, and a decrease in thermal conductivity causes a decrease in heat transfer between fluids in the tube.

It can be seen from Fig. 21 that the turbulent viscosity gradually decreases from the center position in the radial direction, and the wall surface reaches a minimum value. The decrease of the turbulent viscosity reduces the radial turbulent flow energy, which reduces the radial blending heat transfer capacity. . It can be seen in the radial distribution of density in Fig. 22 that the density at $L = 2.5\text{m}$ is significantly smaller than the fluid density at $L = 1.1\text{m}$. The distribution pattern of radial density is still parabolic, and the high temperature at the wall makes the density relatively Smaller.

Based on the analysis of the above situations, we can see that $RNGk - \varepsilon$ Distribution of radial parameters calculated by turbulence model and $k - \varepsilon$ The distribution of the radial parameters calculated by the turbulence model is basically the same.

Combining the calculation results of the two calculation models, the following conclusions can be drawn: the strong buoyant lift effect of the fluid near the wall surface changes the radial flow field structure, the turbulent viscosity at the wall surface decreases, and the thickness of the boundary layer increases accordingly, At the same time, the thermal conductivity and constant pressure specific heat inside the fluid near the wall surface are also reduced, which further reduces the heat transfer coefficient, resulting in a sudden rise in wall temperature and deterioration in heat transfer. Due to the large radial temperature gradient, the turbulent viscosity will gradually decrease, and the turbulent energy of the fluid will be converted into the kinetic energy of the fluid, which will reduce the degree of radial mixing and reduce the heat transfer effect. Boundary layer flow laminarization caused by fluid acceleration in a vertically rising tube is the main cause of this deterioration of heat transfer.

4. The Temperature Field Analysis

Temperature stratification refers to the temperature gradient of the fluid in the radial or axial direction. For circumferentially heat-exchanging pipes, due to the viscosity and other characteristics of the fluid, there is a gradient of flow velocity perpendicular to the direction of the pipe. The change rule is basically center symmetry. And the direction of heat transfer also makes the temperature inside the pipe different. Because the fluid at the wall surface directly contacts the wall surface, the fluid temperature is the highest. The closer to the center of the pipe, the fluid temperature will gradually decrease. At the same time, due to the constant exchange of heat along the flow direction, there will be a gradient change in the fluid temperature.

The existence of temperature stratification will cause the physical properties of the tube to be stratified, and the temperature rises fastest at the wall surface. The physical properties of the coolant will first enter the quasi-critical zone, and then there will be drastic changes, and extreme values of specific volume and viscosity will occur. It will decrease, hinder heat exchange, and due to the weakening of heat conduction, temperature stratification will be exacerbated. However, drastic changes in physical properties will also affect the flow in the tube. Due to the density difference, there will be non-mainstream flow, which will change the mixing state in the tube and enhance heat transfer. Therefore, the axial temperature map and the longitudinal section temperature map at $L = 1\text{m}$, $L = 1.5\text{m}$, $L = 2\text{m}$, $L = 2.5$, and $L = 3\text{m}$ are extracted, and the drawing scale is $Z: X = 100: 1$.

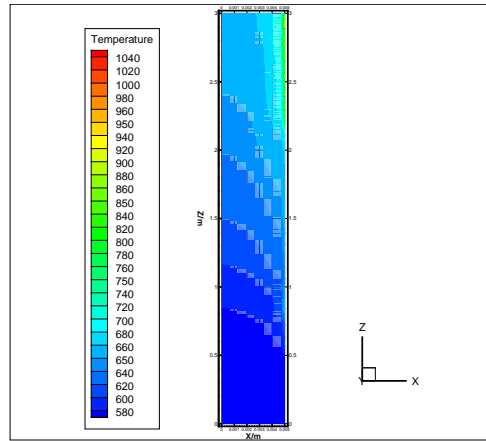


Figure 23 Axial temperature cloud diagram of the pipeline

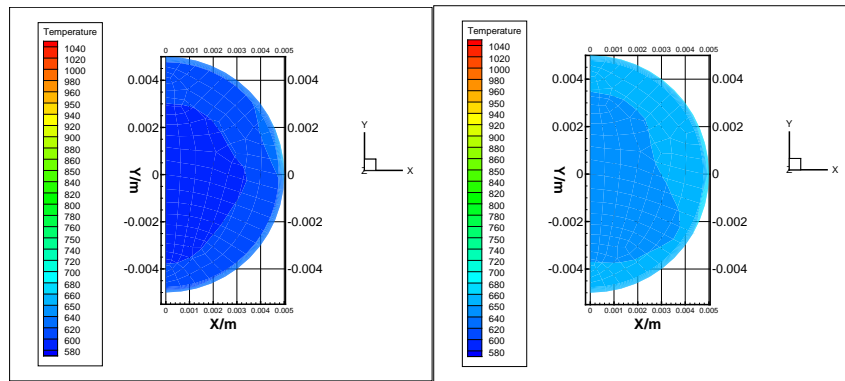


Figure 24 Longitudinal temperature cloud at $L = 1\text{m}$ Figure 25 Longitudinal temperature cloud at $L = 2\text{m}$

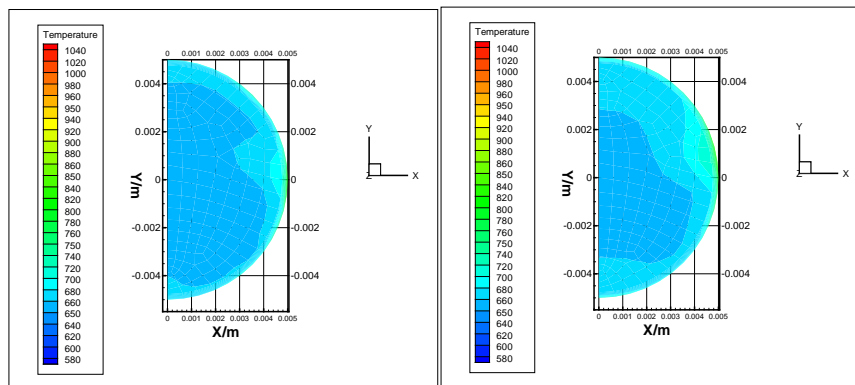


Figure 26 Vertical temperature cloud at $L = 2.5\text{m}$ Figure 27 Longitudinal temperature cloud at $L = 3\text{m}$

It can be seen from the temperature cloud diagram of the axial section of the pipe in Figure 24 that there is a significant temperature gradient along the axial flow direction, mainly because as the water in the pipe flows, the heat transferred from the wall surface to the core flow gradually increases, so the temperature of the fluid increases gradually in the axial direction. It can be seen from Figs. 25 to 28 that in the longitudinal section, there is also obvious temperature stratification in the tube. The main reason is that the fluid at the wall absorbs the heat first to heat up, and it will transmit heat to the internal fluid while continuously absorbing the heat. However, the thermal conductivity of water is limited, so the heat transferred to the interior is limited. Heat absorption at the surface, which leads to the temperature stratification between the core flow and the fluid at the wall surface. The existence of the temperature stratification will increase the heat transfer thermal resistance. The longitudinal sections at $L = 2.5\text{m}$ and $L = 3\text{m}$ can also be seen here. At this time, the temperature stratification at the wall surface has intensified, which is also the cause of the high

temperature on the wall surface.

The existence of the temperature seal layer increases the heat transfer heat resistance, making the physical heat sink of the fluid unable to be completely released, and the heat transfer effect is affected. Therefore, it is necessary to find a method to weaken it. By increasing the roughness in the tube, the blending and mixing between the internal fluids are enhanced. Radial perturbations can be used to weaken the temperature stratification method, but the corresponding will also have negative effects, such as increased flow resistance, increased manufacturing costs and other issues, so further analysis and research are needed.

5. Conclusion

Use higher calculation accuracy $k-\varepsilon$ and $RNGk-\varepsilon$. The turbulence model is simulated under high heat flux density and mass flow conditions. Under the conditions of high heat flux density and high quality flow rate, when the working fluid in the tube enters the heating section, both models can predict the trend of temperature change in the tube with an error value not higher than 10%. As the wall temperature increases, the difference between the calculated results and the experimental data increases, and the error value exceeds 10%, which is close to 100K. and $k-\varepsilon$. The model has a poor prediction trend in the area where the wall temperature rises, and there is a large temperature change, with a range of nearly 200K. $RNGk-\varepsilon$. Although the turbulence model has temperature fluctuations, the range does not exceed 100K, and the prediction accuracy is higher.

By analyzing the axial and radial parameters in the tube, it is concluded that when the physical properties change sharply when entering the critical region, the heat transfer coefficient decreases and the viscous bottom layer at the wall surface thickens. With the flow heat transfer in the tube, the viscous bottom layer increased from about 0.2mm to about 1mm. The increase of the viscous bottom layer causes a relatively large change in physical properties at the wall surface, a sudden change in specific heat value, and a sharp decrease in thermal conductivity, leading to a decrease in heat transfer effect and an increase in wall temperature of nearly 300K.

By analyzing the temperature field distribution in the tube, it can be seen that there are obvious temperature gradients in the axial and radial directions inside the circumferentially heat-exchanging tube. In the area of deteriorated heat transfer, the radial temperature gradient will intensify, especially at the viscous bottom layer of the wall surface, and the temperature difference within 1mm will reach 300K. The existence of a temperature gradient prevents the physical enthusiasm of the fluid in the tube from being completely released. Therefore, weakening the temperature gradient can be studied as one of the methods to enhance heat transfer.

References

- [1]. Singh P.M., Mahmood J. Stress corrosion cracking of Type 304L stainless steel in sodium sulfide-containing caustic solutions. *Corrosion*, 2003, 843-850
- [2]. Hua Yongming, Zhou Qiangtai. Theoretical study on the stress characteristics of 1025t / h once-through boiler water-cooled wall. *Boiler Technology*, 2000, 11-15
- [3]. Zhao Minfu, Zhang Guoxin, Chen Yuzhou. Numerical simulation of heat transfer characteristics of supercritical water in vertical round tubes [J]. *Atomic Energy Science and Technology*, 2011, 02: 146-149.
- [4]. Cheng X, Schulenberg T. Heat transfer at supercritical pressures-literature review and application to a HPLWR, FZKA 6609 [R]. Karlsruhe, Germany: FZKA, 2001.
- [5]. Wang Lei. Research on heat transfer characteristics of supercritical water in vertical circular tubes [D]. Shanghai Jiaotong University, 2012.
- [6]. Yuying Ying, Fuxiang Zhang. Comparison of layout types of supercritical once-through boiler water-cooled wall. *Power Engineering*, 2008, 28: 333 ~ 338

- [7]. Xu Feng, Study on Water Flow and Heat Transfer Characteristics in Supercritical Pressure Tube, Xi'an Jiaotong University Master's Degree Thesis, 2004.
- [8]. I.L.Pioro, R.B.Duffey. Experimental heat transfer in supercritical water flowing inside channels (survey) [J]. Nuclear Engineering and Design, 2005, 235(22): 2407 — 2430.
- [9]. Ge Zhang, Hao Zhang, Hanyang Gu, Yanhua Yang, Xu Cheng, Experimental and numerical investigation of turbulent convective heat transfer deterioration of supercritical water in vertical tube. Nuclear Engineering and Design, Volume 248, July 2012, Pages 226-237.
- [10]. Mokry S, Farah A., King K. and Pioro I.L. Updated heat-transfer correlations for supercritical water-cooled reactor applications. The 5th Int. Sym. SCWR (ISSCWR-5) Vancouver, British Columbia, Canada, March. 2011, 13-19.
- [11]. Wang Yingjie. Review of heat transfer characteristics of supercritical fluids [J]. Science & Technology Review. 2012, v. 30; 779.
- [12]. Cheng X., Kuang B. and Yang Y.H. Numerical analysis of heat transfer in supercritical water-cooled flow channels [J]. Nuclear Engineering and Design, 2007, 237: 240–252.
- [13]. Z.Shang, Y.E.Yao, S.Chen. Numerical investigation of system pressure effect on heat transfer of supercritical water flows in a horizontal round tube [J]. Chemical Engineering Science, 2008, 63(16): 4150 — 4158.
- [14]. Shi Xiaobao, Wang Haijun, Luo Yushan, Li Hongzhi. Numerical Analysis of Heat Transfer of Supercritical Water in Vertically Rising Circular Tube [J]. Journal of Jishou University (Natural Science Edition), 2008, (06): 50-54.
- [15]. Bo Zhang, Jianqiang Shan, Jing Jiang, Numerical analysis of supercritical water heat transfer in horizontal circular tube, Progress in Nuclear Energy, Volume 52, Issue 7, September 2010: 678-684.
- [16]. Lei Xianliang, Li Huixiong, Yu Shuiqing, Ren Dalong. Numerical simulation of non-uniform heat transfer characteristics of supercritical water in inclined rising tube [J]. Chinese Journal of Computational Physics, 2010, (02): 217-228.
- [17]. Huang Zhigang, Li Yongliang, Zeng Xiaokang, Yan Xiao, Xiao Zejun. Experimental and numerical simulation of heat transfer in supercritical water in vertical tube passages [J]. Atomic Energy Science and Technology, 2012, (07): 799-803.
- [18]. Huang Zhigang, Zeng Xiaokang, Li Yongliang, Yan Xiao, Xiao Zejun. Numerical simulation and model evaluation of heat transfer deterioration of supercritical water in a circular tube [J]. Nuclear Power Engineering, 2012, (02): 66-70.
- [19]. Jan A.M. Withag, Joost L.H.P. Salleveld, Derk W.F. Brilman, Eddy A. Bramer, Gerrit Brem, Heat transfer characteristics of supercritical water in a tube: Application for 2D and an experimental validation, The Journal of Supercritical Fluids, Volume 70, October 2012, Pages 156-170.
- [20]. Maria Jaromin, Henryk Anglart, A numerical study of heat transfer to supercritical water flowing upward in vertical tubes under normal and deteriorated conditions, Nuclear Engineering and Design, Available online 21 March 2013, ISSN 0029-5493, 10.1016/j.nucengdes.2012.10.028.
- [21]. Xiong Lifang, Lin Yuan, Li Shiwu. Turbulence model and its application in FLUENT software [J]. Industrial Heating, 2007, 04: 13-15.
- [22]. Ruan B, Meng H. Supercritical Heat Transfer of Cryogenic-Propellant Methane in Rectangular Engine Cooling Channels [J]. Journal of Thermophysics and Heat Transfer, 2012, 26(2): 313-321.